Synthetic Metals 252 (2019) 127–134

Contents lists available at ScienceDirect

Synthetic Metals

journal homepage: www.elsevier.com/locate/synmet

Synthesis and properties of a P3HT-based ABA triblock copolymer containing a perfluoropolyether central segment

Michèle Chevrier[a,b], Gérald Lopez[a], Wojciech Zajaczkowski[c], Jurgen Kesters[d], Ruben Lenaerts[d], Mathieu Surin[e], Julien De Winter[f], Sébastien Richeter[a], Wojciech Pisula[c,g], Ahmad Mehdi[a], Pascal Gerbaux[f], Roberto Lazzaroni[e], Philippe Dubois[b], Wouter Maes[d], Bruno Ameduri[a,*], Sébastien Clément[a,*]

[a] Institut Charles Gerhardt, Université de Montpellier, Place Eugène Bataillon, 34095 Montpellier Cedex 05, France
[b] Service des Matériaux Polymères et Composites (SMPC), Centre d'Innovation et de Recherche en Matériaux et Polymères (CIRMAP), Université de Mons - UMONS, Place du Parc 20, 7000 Mons, Belgium
[c] Max Planck Institute for Polymer Research, Ackermannweg 10, 55128 Mainz, Germany
[d] Institute for Materials Research (IMO), Design & Synthesis of Organic Semiconductors (DSOS), Hasselt University-UHasselt, Agoralaan 1–Building D, B-3590 Diepenbeek, Belgium
[e] Laboratory for Chemistry of Novel Materials, Center of Innovation and Research in Materials and Polymers (CIRMAP), University of Mons UMONS, Place du Parc 20, 7000 Mons, Belgium
[f] Organic Synthesis & Mass Spectrometry Laboratory, Interdisciplinary Center for Mass Spectrometry (CISMa), Center of Innovation and Research in Materials and Polymers (CIRMAP), University of Mons – UMONS, 23 Place du Parc, 7000, Mons, Belgium
[g] Department of Molecular Physics, Faculty of Chemistry, Lodz University of Technology, Zeromskiego 116, 90-924 Lodz, Poland

ARTICLE INFO

Keywords:
Block copolymer
Poly (3-hexylthiophene)
Perfluoropolyether
Bulk heterojunction
Organic solar cells

ABSTRACT

A poly(3-hexylthiophene)-*block*-perfluoropolyether-*block*-poly(3-hexylthiophene) (P3HT-*b*-PFPE-*b*-P3HT) triblock copolymer was synthesized by copper(I)-catalyzed alkyne–azide cycloaddition (CuAAC) in 95% yield. The copolymer was unequivocally characterized by size exclusion chromatography reaching 27 000 g mol^{-1} and nuclear magnetic resonance (NMR). As expected, diffusion-ordered spectroscopy NMR experiment revealed a lower diffusion coefficient (2.56×10^{-10} $m^2 s^{-1}$) for the P3HT-*b*-PFPE-*b*-P3HT triblock copolymer than the ethynyl end-functionalized P3HT (2.83×10^{-10} $m^2 s^{-1}$). Such a triblock copolymer exhibits i) a good thermal stability with no significant weight loss until 320 °C under air, ii) a glass transition of -50 °C due to the soft PFPE segment and iii) a melting peak arising from P3HT at 236 °C. The UV–vis absorption spectrum exhibits a similar absorption profile to that of pure P3HT with a vibronic structure. Analysis of terpolymer thin films by atomic force microscopy imaging and grazing incidence wide-angle X-ray scattering reveals the formation of P3HT crystallites and an "edge-on" orientation of the polymer chains towards the substrate. Preliminary photovoltaic studies on blends of this triblock copolymer combined with a fullerene derivative indicate that the devices using P3HT-*b*-PFPE-*b*-P3HT show an almost similar power conversion efficiency to commercial P3HT.

1. Introduction

Conjugated semiconducting polymers have become unavoidable materials in active layers in organic electronics such as organic photovoltaics (OPVs), organic light-emitting diodes (OLEDs) and organic thin-film transistors (OTFTs) [1–4]. Among these materials, poly(3-hexylthiophene) (P3HT) is certainly the most studied due to its well-balanced properties in terms of solubility, environmental/thermal stabilities and charge carrier transport, but also and above all, its synthetic availability [5–8]. Indeed, P3HTs with multiple architectures (homopolymers, random/block copolymers) and an excellent control over the molecular weight (M_w), molecular weight distribution (Đ) and regioregularity (RR) can readily be obtained via catalyst-transfer polymerization [5,9]. Many studies have shown that the molecular packing and nanoscale morphology of P3HT determine its optoelectronic properties and thus, strongly influence the corresponding electronic applications [10,11]. Therefore, the control of the P3HT nanostructuration in the solid state have been pursued to achieve optimal device performance.

Block copolymers are interesting materials to generate suitable

* Corresponding authors.
E-mail addresses: bruno.ameduri@enscm.fr (B. Ameduri), sebastien.clement1@umontpellier.fr (S. Clément).

https://doi.org/10.1016/j.synthmet.2019.04.001
Received 2 January 2019; Received in revised form 21 March 2019; Accepted 2 April 2019

morphologies for optoelectronic applications due to their ability to self-assemble into ordered, periodic structures at the length scale of the individual polymer chains [12,13]. In this respect, many block copolymers containing P3HT segment(s) were developed in particular, those combining a non-conjugated block (coil) and a P3HT (rod) block. To date, a wide variety of "coil-like" segments such as poly(styrene) [14–16], poly(allene), [17,18] poly(urethane) [14], poly-phthalaldehyde [19], poly(methyl methacrylate) [20–22], poly(4-vinylpyridine) [23,24], poly(ε-caprolactone) [25], polylactide [26], poly (dimethoxysilane) [27] and poly(ethylene glycol) [28,29] have been exploited to tune the crystallinity of the materials and their film morphology. Among rod-coil block copolymers, ABA-type rod-coil-rod block copolymers have rarely been investigated although they can provide new opportunities for directing self-assembly through inter- and intrachain interactions [18,30,31]. Such P3HT triblock copolymers can also possess improved mechanical properties, similar to ABA triblock copolymer thermoplastic elastomers (TPEs), such as polystyrene-*block*-polybutadiene-*block*-polystyrene (SBS) [32].

Introducing a fluorinated segment as the coil block in a rod-coil block copolymer also allows manipulating the solid-state organization. Indeed, the immiscibility with hydrocarbon groups and the F···π, F···H and F···S inter- and intramolecular interactions may have a significant role in the self-assembly of the block copolymers in the solid-state [33–35]. Incorporated as the coil segment into rod-coil block copolymers, fluorinated moieties may impart their unique properties (e.g. chemical inertness, hydrophobicity, and high thermal and oxidation stability) [36,37]. Along that line, Mc Cullough et al. have shown that the attachment of a hydrophobic poly(fluorinated alkyl methacrylate) coil allows to significantly improve the charge carrier transport properties of regioregular poly(3-hexylthiophene) (rr-P3HT) [38]. The presence of fluorinated chains may also have a positive impact on the interfacial area between the donor and the acceptor as well as to provide bicontinuous networks of donor and acceptor domains in bulk heterojunction organic solar cells, leading to enhanced percolation pathways for charge transport and thus, better power conversion efficiencies [39–41].

In this work, a telechelic bisazide fluorinated polyether is covalently attached by copper(I)-catalyzed alkyne–azide cycloaddition (CuAAC) to an ethynyl end-functionalized regioregular P3HT, forming a rod-coil-rod triblock copolymer (P3HT-*b*-PFPE-*b*-P3HT). The thin film microstructure of the P3HT-*b*-PFPE-*b*-P3HT copolymers is investigated using grazing incidence wide-angle X-ray scattering (GIWAXS) and atomic force microscopy (AFM). P3HT rod blocks self-assemble into highly ordered lamellar configurations, similar to rr-P3HT homopolymers. Device evaluation of photovoltaic cells based on P3HT-*b*-PFPE-*b*-P3HT blended with [6,6]-phenyl-C61-butyric acid methyl ester ($PC_{61}BM$) reveals triblock copolymer only slightly underperforms as compared to commercial P3HT.

2. Materials and experimental method

2.1. Materials

All reactions were carried out under an atmosphere of dry argon. THF was dried using a solvent purification system PureSolve MD5 from Innovative Technology with alumina drying columns. 2-Bromo-3-hexyl-5-iodothiophene, [42] (*o*-tolyl)Ni(PPh_3)$_2$Br [43,44], telechelic PFPE-–bisazide were synthesized following reported procedures [45,46]. Isopropylmagnesium chloride (2.0 M in THF), 1,3-bis(diphenylphosphino) propane (dppp, 97%), ethynylmagnesium chloride (0.5 M in THF), copper(I) bromide (98%) and *N,N,N′,N′,N″*-pentamethyldiethylenetriamine (PMDETA, 99%) were purchased from Aldrich. P3HT (M_n = 25 000 g mol^{-1}, M_w = 31 000 g.mol^{-1}, Đ = 1.24) was prepared as previously described [47,48]. Commercial P3HT (M_w = 50 000–70 000 g.mol^{-1}) was obtained from Solarmer. [6,6]-phenyl-C_{61}-butyric acid methyl ester ($PC_{61}BM$) (99%) was purchased from Solenne BV. Reagent Plus grade methanol (> 99%, Aldrich), ACS reagent grade chlorobenzene (99.5%, Aldrich), reagent grade xylene (98.5%, Aldrich) and HPLC grade *o*-dichlorobenzene (*o*-DCB) (99%, Aldrich) were used without further purification. Deuterated chloroform ($CDCl_3$), used for NMR spectroscopy, was purchased from Euriso-top (purity > 99.8%).

2.2. Techniques

The NMR spectra of the polymers were collected at 25 °C on a Bruker Avance III 400-MHz spectrometer equipped with two independent broadband (^{15}N–^{31}P and ^{15}N–^{19}F, 300 W) and a high band (^{1}H, 100 W) rf channel. A 5 mm $^{1}H/^{19}F/^{13}C$ TXO triple resonance pulsed field gradient probe for which ^{13}C and ^{19}F are on the inner coil and ^{1}H on the outer coil is used for three-channel experiments. This triple resonance $^{1}H/^{19}F/^{13}C$ probe has a lower background ^{19}F signal compared to standard dual-channel probes, and is capable of producing short 90° pulses (6.5 µs for ^{19}F, 9.5 µs for ^{13}C and 9.2 µs for ^{1}H). Diffusion-ordered NMR spectroscopy (DOSY) experiments were performed as previously described [45].

Size exclusion chromatography (SEC) measurements were performed on a Polymer Laboratories liquid chromatograph equipped with a PL-DG802 degasser, an isocratic HPLC pump LC 1120 (flow rate of THF of 1 mL min^{-1}), a Marathon autosampler (loop volume of 200 mL, solution concentration of 1 mg mL^{-1}), a PL-DRI refractive index detector, and three columns: a PL gel 10 mm guard column and two PL gel Mixed-B 10 mm columns (linear columns for the separation of polystyrene standards with molecular weight ranging from 500 to 10^6 Da). Polystyrene was used as standard for calibration.

Matrix-assisted laser desorption/ionization time-of-flight (MALDI-ToF) mass spectra were recorded using a Water QToF Premier mass spectrometer equipped with a Nd:YAG (third harmonic) operating at 355 nm with a maximum output of 65 µJ delivered to the sample in 2.2 ns pulses at 50 Hz repeating rate. Time-of-flight mass analyses were carried out in the reflectron mode at a resolution of about 10 000. All samples were analyzed using *trans*-2-[3-(4-*tert*-butylphenyl)-2-methyl-prop-2-enylidene]malononitrile (DCTB) as matrix, which was prepared as a 40 mg mL^{-1} solution in $CHCl_3$ [49]. The matrix solution (1 mL) was applied to a stainless steel target and air dried. Polymer samples were dissolved in $CHCl_3$ to obtain 1 mg mL^{-1} solutions. 1 µL aliquots of these solutions were applied onto the target area already bearing the matrix crystals and air dried. For the recording of the single-stage MS spectra, the quadrupole (rf-only mode) was set to pass ions from *m/z* 500 to *m/z* 15 000, and all ions were transmitted into the pusher region of the time-of-flight analyzer where they were mass-analyzed with 1 s integration time.

Thermogravimetric measurements were performed on a TA Instruments TGA 51 thermogravimetric analyzer in air, at a heating rate of 10 °C min^{-1} from room temperature up to a maximum of 600 °C. Differential scanning calorimetry (DSC) measurements (TA instruments Q100) were performed under an atmosphere of nitrogen at a heating/cooling rate of 10 °C min^{-1}. The sample size varied between 10 and 15 mg. UV/vis absorption spectra were recorded with a JASCO V-650 UV–visible spectrophotometer.

The atomic force microscopy (AFM) measurements were performed on an Icon Bruker microscope in tapping mode. The samples were drop casted from xylene solution (0.1 mg mL^{-1}) of the polymer onto mica substrates and then, placed under saturation in xylene vapor for 16 h.

(GIWAXS) measurements of the thin films were made using a custom setup consisting of copper solid-anode X-ray tube (Bruker AXS Krystalloflex 760, operated at 35 kV and 30 mA), Osmic confocal MaxFlux optics and a three pin-hole collimation system. The X-ray beam size has 1.0 mm radius, and samples were irradiated just below the critical angle for total reflection with respect to the incoming X-ray beam (~0.1°). The scattering intensity was detected on a 2D image plate (MAR-345) with a pixel size of 100 µm (2345 × 2345 pixels), and the detector was placed 300 mm from the sample center. Scattering

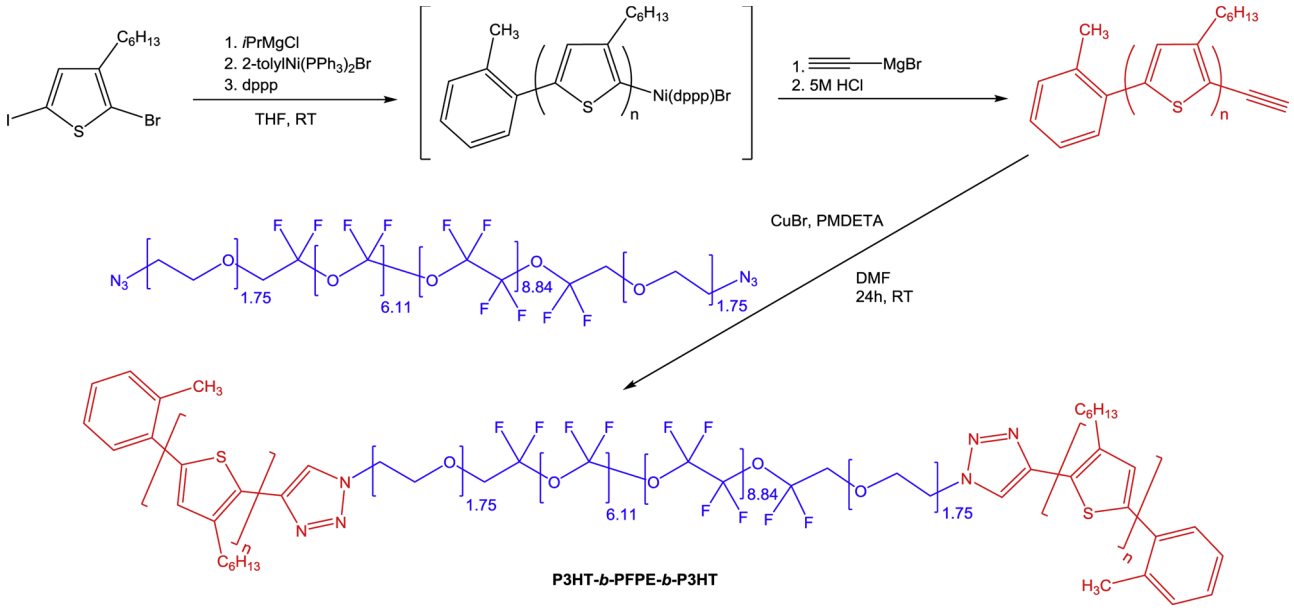

Scheme 1. Synthesis of the P3HT-*b*-PFPE-*b*-P3HT triblock copolymer from the Huisgen reaction between an ethynyl end-functionalized P3HT and a telechelic bis-azido perfluoropolyether (PFPE).

data are expressed as a function of the scattering vector: q = 4π/λ sin (Θ), where Θ is a half the scattering angle and λ = 1.54 Å is the wavelength of the incident radiation. Here, qxy (qz) is a component of the scattering vector in plane (out-of-plane) to the sample surface. All X-ray scattering measurements were performed under vacuum (~1 mbar) to reduce air scattering and beam damage to the sample. All GIWAXS data processing and analysis were performed by using the software package Datasqueeze (http://www.datasqueezesoftware.com).

2.3. Solar cell fabrication and characterization

Bulk heterojunction organic solar cells were prepared using the conventional architecture consisting of glass/ITO/PEDOT:PSS/active layer/Ca/Al. Before device processing, the indium tin oxide (ITO, Kintec, 100 nm, 20 Ω sq^{-1}) coated substrates were subjected to a standard cleaning procedure using soap, demineralized water, acetone, isopropanol, and a UV/O_3 treatment. PEDOT:PSS [poly(3,4-ethylenedioxythiophene):poly(styrenesulfonic acid), Heraeus Clevios] was then deposited via spin-coating to obtain a layer thickness of ~30 nm, followed by a thermal treatment of 15 min at 130 °C to remove any residual water. Further processing was performed in a nitrogen-filled glove box (O_2 /H_2O < 0.1 ppm). The photoactive polymer:$PC_{61}BM$ blend in a 1.2:1 (wt:wt%) ratio was then spin-coated from a 40 mg mL^{-1} solution in *ortho*-dichlorobenzene. The photoactive layers were annealed at 140 °C for 5 min after spin-coating. To complete the fabrication of the devices, Ca and Al electrodes were deposited with a thickness of ~30 and ~80 nm, respectively. The I–V characteristics were determined using a Newport Class A solar simulator (model 91195A), calibrated with a silicon solar cell to give an AM 1.5 G spectrum. External quantum efficiencies (EQEs) were determined by recording the monochromated (Newport Cornerstone 130 with sorting filters) output of a xenon lamp (100 W, Newport 6257) by a lock-in amplifier (Stanford Research Systems SR830). The recorded values were calibrated with an FDS-100 calibrated silicon photodiode.

2.4. Synthesis

2.4.1. Synthesis of the ethynyl end-functionalized P3HT

Dry THF (15.0 mL) was added via a syringe into a flask containing 2-bromo-3-hexyl-5-iodothiophene (1.90 g, 5.11 mmol) under a nitrogen atmosphere, and the mixture was stirred at 0 °C. *i*PrMgCl (2.0 M solution in THF, 2.55 mL, 5.11 mmol) was added via a syringe, and the mixture was stirred at 0 °C for 0.5 h. At the same time, a suspension of (*o*-tolyl)$Ni(PPh_3)_2Br$ (27.40 mg, 0.04 mmol) and dppp (30.05 mg, 0.08 mol) in THF (15.0 mL) was stirred at room temperature for 15 min. To this suspension, the monomer solution was added and the mixture was stirred at 0 °C for 3 h. Ethynylmagnesium bromide (25 mol %) was injected all at once and the mixture was stirred for another 5 min. The mixture was then injected into methanol and the suspension was stirred for 30 min. The resulting product was filtered, washed with MeOH and dried under vacuum yielding a purple solid. Yield: 71%. ^{1}H NMR (400 MHz, $CDCl_3$): δ = 6.98 (s, 47 H), 6.97 (d, $^3J_{H-H}$ = 8.0 Hz, 2 H), 6.90 (d, $^3J_{H-H}$ = 8.0 Hz, 2 H), 3.53 (s, 1H, C≡CH), 2.80 (t, $^3J_{H-H}$ = 8.0 Hz, 94 H), 2.50 (s, 3H, CH_3), 1.71 (quint, $^3J_{H-H}$ = 8.0 Hz, 94 H), 1.45-1.27 (m, 282 H), 0.91 (t, $^3J_{H-H}$ = 6.0 Hz, 141 H) ppm; SEC analysis (THF) : M_n = 13150 g/mol; Đ = 1.16.

2.4.2. Synthesis of the P3HT-b-PFPE-b-P3HT triblock copolymer

Telechelic PFPE–bisazide (70 mg, 0.035 mmol, 1 eq.) and ethynyl end-functionalized P3HT (500 mg, 0.07 mmol, 2 eq.) were suspended in DMF (10 mL). The mixture was degassed by bubbling nitrogen for 30 min. Then, copper(I) bromide (CuBr, 0.50 mg, 0.0035 mmol, 0.1 eq.) and *N,N,N′,N″,N″*-pentamethyldiethylenetriamine (PMDETA, 0.60 mg, 0.0035 mmol, 0.1 eq.) were added into the reaction mixture. After stirring at room temperature for 24 h, the reaction mixture was added dropwise into cold methanol. After filtration, the slightly green powder was dried under vacuum until constant weight. Yield: 95%. ^{1}H NMR (400 MHz, $CDCl_3$): δ = 7.75 (s, 2 H), 6.98 (s, 128 H), 6.97 (d, $^3J_{H-H}$ = 8.0 Hz, 4 H), 6.90 (d, $^3J_{H-H}$ = 8.0 Hz, 4 H), 4.68-4.60 (m, 4 H), 4.15-3.28 (m, 14H, CH_2), 2.80 (t, $^3J_{H-H}$ = 8.0 Hz, 256 H), 2.50 (s, 6H, CH_3), 1.71 (quint, $^3J_{H-H}$ = 8.0 Hz, 256 H), 1.45-1.27 (m, 768 H), 0.91 (t, $^3J_{H-H}$ = 6.0 Hz, 384 H) ppm; ^{19}F NMR (376.4 MHz, $CDCl_3$): δ = -53 (OCF_2), -78 (OCF_2CH_2), -90 (OCF_2CF_2) ppm; $^{13}C\{^1H\}$ NMR (100.6 MHz, $CDCl_3$): δ = 140.1, 133.1, 130.6, 128.4, 31.8, 30.4, 29.4, 29.4, 22.8, 14.3 ppm; SEC analysis (THF) : M_n = 27000 g/mol; Đ = 1.36.

3. Results and discussion

3.1. Synthesis and characterization of P3HT-b-PFPE-b-P3HT

Ethynyl end-functionalized regioregular P3HT was first synthesized through the externally-initiated Kumada catalyst transfer polymerization (KCTP) of 2-bromo-3-hexyl-5-iodothiophene using a σ-aryl nickel initiator ((2-tolyl)Ni(PPh_3)$_2$Br) [50,51] and its quenching with ethynylmagnesium chloride (Scheme 1).

To avoid end-group degradation, no Soxhlet extraction was performed to remove low-molecular weight fractions [19,52]. As such, a number-averaged molecular weight (M_n) of 13 150 g mol^{-1} and a dispersity (Đ) of 1.16 were obtained from the monomodal trace of the ethynyl end-functionalized P3HT polymer in the SEC analysis (Figure S1 in the Supporting Information). To identify polymer end-groups, MALDI-ToF mass spectrometry was used (Figure S2 in the Supporting Information). The polymer shows a major distribution of o-tolyl/acetylene end groups and few o-tolyl/Br end groups (not involved in the envisaged click reaction). An average molecular weight of 9 000 g mol^{-1} is approximated by MALDI. Such a difference between the molecular weights obtained by SEC and MALDI is not unusual since SEC analysis using PS calibration usually overestimates the molecular weight of rigid-rod P3HT by a factor of 1.2–2.3 [49,53]. A singlet at δ = 3.53 ppm, corresponding to the alkyne proton (−C≡CH) (Figure S3 in the Supporting Information) is also observed by ^{1}H NMR spectroscopy. The molecular weight of the end-functionalized P3HT was also estimated from its ^{1}H NMR spectrum (Figure S3 in the Supporting Information). The peaks observed at δ = 2.80 and 2.50 ppm are assigned to the resonance of α-methylene group of the P3HT side chains and the methyl group of the *o*-tolyl initiator, respectively. From the integration of these two peaks, the number of 3HT units was found to be 40, corresponding to an average molecular weight of ~ 7 000 g mol^{-1}, that confirms the mass range estimated by MALDI mass spectrometry.

The fluorinated coil of the ABA triblock copolymer was obtained by using fluorolink E10H a telechelic PFPE-diol, abbreviated E10H (~1 800 g.mol^{-1}), marketed by Acota Company that was chemically modified by tosylation then azidation, as previously described. [46] PFPE-bisazide and ethynyl end-functionalized P3HT were then covalently coupled via click chemistry to afford the P3HT-*b*-PFPE-*b*-P3HT triblock copolymer (Scheme 1). To ensure the complete consumption of the reactive species, copper(I)-catalyzed alkyne-azide cycloaddition (CuAAC) was performed using two equivalents of P3HT-alkyne compared to PFPE-bisazide. Copper(I) bromide (0.1 mol eq.) and *N,N,N′,N′,N′′*-pentamethyldiethylenetriamine (PMDETA, 0.1 mol eq.) were employed as the catalyst and the ligand, respectively. After one day-reaction at room temperature, the P3HT-*b*-PFPE-*b*-P3HT triblock copolymer was recovered by precipitation in cold methanol (95 wt.% yield). The appearance of the triazole protons that resonate at δ = 7.75 ppm in the ^{1}H NMR spectrum of the triblock copolymer (Fig. 1, signal c) provides evidence of a successful click reaction. The characteristic signals of PFPE [45] (i.e., O−CH_2CH_2- (Fig. 1, signal b) and CF_2−CH_2-O (Fig. 1, signal a) are also present along with those of P3HT. The ^{19}F NMR spectrum of the P3HT-*b*-PFPE-*b*-P3HT triblock copolymer (Figure S4 in the Supporting Information) displays the signals typically attributed to PFPEs (i.e. OCF_2, OCF_2CH_2 and OCF_2CF_2 centered at δ = -53, -78 and -90 ppm, respectively). The ^{13}C{^{1}H} NMR spectrum of the P3HT-*b*-PFPE-*b*-P3HT triblock copolymer (Figure S5 in the Supporting Information) exhibits the characteristic signals of P3HT, whereas those attributed to the PFPE segment are too weak to be identified. SEC analysis of the isolated material reveals a monomodal trace recorded at lower elution volume (higher M_n) than the ethynyl end-functionalized P3HT (Figure S1 in the Supporting Information), indicating a successful coupling reaction. The measured M_n of the triblock copolymer is 27 000 g mol^{-1}, which is very close to the sum (M_n = 28 100 g mol^{-1}) of the M_n of the ethynyl end-functionalized P3HT precursor (M_n = 13 150 g mol^{-1}) and the PFPE-bisazide (M_n = 1 800 g mol^{-1}). The formation of the triblock copolymer is also confirmed by diffusion-ordered ^{1}H NMR spectroscopy (^{1}H DOSY) (Fig. 2). As expected, the lower molar mass ethynyl end-functionalized P3HT precursor has a higher diffusion coefficient (2.83 × 10^{-10} m^2 s^{-1}) whereas the higher triblock copolymer has a lower diffusion coefficient (2.56 × 10^{-10} m^2 s^{-1}).

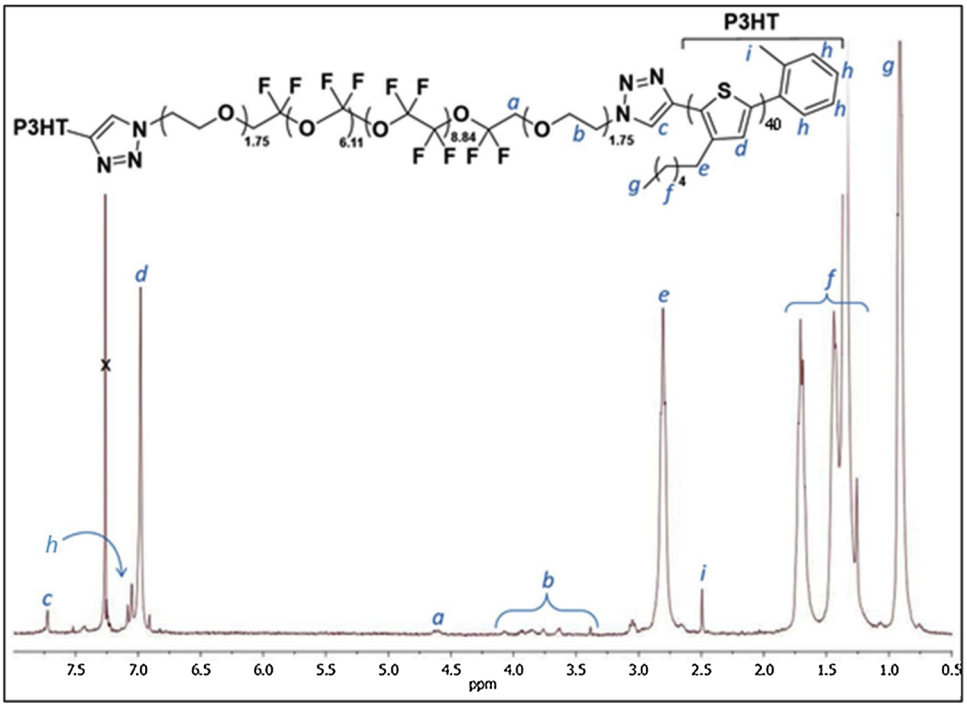

Fig. 1. ^{1}H NMR spectrum of the P3HT-*b*-PFPE-*b*-P3HT triblock copolymer in $CDCl_3$ at 25 °C.

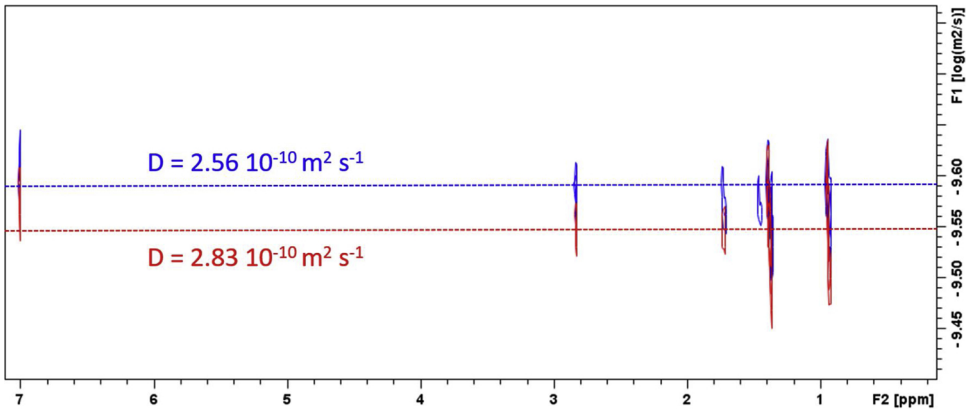

Fig. 2. ^{1}H NMR-DOSY spectra of the P3HT-*b*-PFPE-*b*-P3HT triblock copolymer (top) and ethynyl end-functionalized P3HT precursor (bottom) recorded in $CDCl_3$ at 25 °C (For interpretation of the references to colour in this figure legend, the reader is referred to the web version of this article).

3.2. Thermal, optical and morphological properties of P3HT-b-PFPE-b-P3HT

The thermal properties of the P3HT-*b*-PFPE-*b*-P3HT triblock copolymer were assessed by thermogravimetric analysis (TGA) in air and differential scanning calorimetry (DSC) measurements. The P3HT-*b*-PFPE-*b*-P3HT triblock copolymer displays a multiple-stage decomposition behavior in air (Figure S6 in the Supporting Information) as previously observed for P3HT-based polymers [54,55]. The profile of the decomposition behavior of P3HT-*b*-PFPE-*b*-P3HT is quite similar as that of the P3HT precursor. The onset decomposition temperature of P3HT-*b*-PFPE-*b*-P3HT for a 5% weight loss ($T_{d,5\%}$) is 320 °C, which is somewhat lower than the ethynyl end-functionalized P3HT precursor (Figure S6 in the Supporting Information). This is probably due to the presence of the PFPE block, which is expected to show a lower stability. The DSC thermogram of the triblock copolymer (Figure S7 in the Supporting Information) exhibits a Tg of -50 °C due to the soft PFPE segments and a melting peak arising from P3HT at 236 °C [56,57]. Another transition takes place at higher temperatures (˜ 25 °C); such a phenomenon is also noted in the DSC thermogram of commercially available Fluorolink E10H. This transition is likely to be due either to a mixed phase or to an interphase region, containing both fluorinated and hydrogenated segments [58].

The optical properties of the P3HT-*b*-PFPE-*b*-P3HT triblock copolymer were studied by UV–vis (UV–vis) absorption spectroscopy. The UV–vis absorption spectrum of the P3HT-*b*-PFPE-*b*-P3HT films prepared by drop-casting a 0.5 mg mL^{-1} polymer solution exhibits a similar absorption profile to that of pure P3HT, with an absorption maximum at 558 nm as well as a shoulder at 605 nm (Figure S8 in the Supporting Information) [59]. The presence of this shoulder is attributed to the vibronic progression of the C=C stretching mode (ΔE = 0.15 eV) [60]. This vibronic structure also supports the formation of the P3HT crystalline domains in the film.

In order to further investigate the organization of the P3HT-*b*-PFPE-*b*-P3HT triblock copolymer in thin films, grazing incidence wide-angle X-ray scattering (GIWAXS) studies were performed. The polymer was drop-cast from a 0.15 mg mL^{-1} chlorobenzene solution on a Si/SiO_2 substrate. The solvent was evaporated over 4 h at room temperature. Afterwards the sample was stored at 50 °C overnight to remove residual solvent from the film. The GIWAXS pattern of P3HT-*b*-PFPE-*b*-P3HT in Fig. 3 indicates a typical lamellar organization on the surface as observed for P3HT. The out-of-plane h00 reflections are related to the lamellar structure with an interlayer distance of 1.63 nm, which is similar to the value for pristine P3HT [61,62]. Reflections up to 3rd order indicate long-range arrangement in the out-of-plane direction, but the large azimuthal distribution of the scattering intensities is characteristic for certain misalignment of the domains towards the surface. The wide-angle in-plane 010 reflection is assigned to the π-stacking distance of 0.39 nm [63]. The position of the h00 and 0k0 reflections on specific planes of the pattern is characteristic for an edge-on arrangement of the conjugated polymer backbone on the surface.

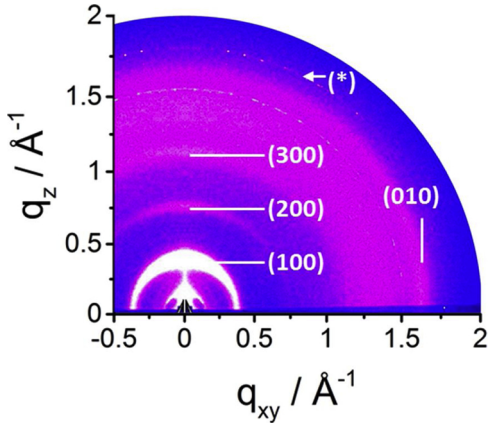

Fig. 3. GIWAXS pattern of the P3HT-*b*-PFPE-*b*-P3HT block copolymer film cast from a chlorobenzene solution (0.15 mg.mL^{-1}). Reflections are assigned by using Miller indexes. (*) Artefact.

Tapping mode AFM images of the topography of P3HT-*b*-PFPE-*b*-P3HT thin films obtained by drop-casting from a 0.1 mg mL^{-1} xylene solution onto mica substrates further support the periodic P3HT nanofibrillar structure in thin films (Fig. 4). This morphological feature is often encountered in regioregular P3HT homopolymers [64–66], and copolymers, suggesting that the organization of P3HT-*b*-PFPE-*b*-P3HT is governed by the self-assembly of P3HT blocks.

3.3. Photovoltaic properties of the P3HT-b-PFPE-b-P3HT triblock copolymer

Preliminary photovoltaic studies were then performed to investigate the behavior of the P3HT-*b*-PFPE-*b*-P3HT triblock copolymer as electron donor material in bulk heterojunction polymer solar cells. Standard architecture devices consisting of glass/ITO/PEDOT:PSS/active layer/Ca/Al were prepared. Photoactive layers consisting of P3HT-*b*-PFPE-*b*-P3HT or synthesized P3 H T (M_n = 25000 g mol^{-1}, Đ = 1.24) as a reference with $PC_{61}BM$ in a 1.2:1 (wt/wt) ratio were spin-coated from *o*-dichlorobenzene. A commercial batch of P3HT (Solarmer) was taken along as well for proper comparison. As summarized in Table 1 and Figure S9 in the Supporting Information, the triblock copolymer performs significantly better than the synthesized P3HT material (which underwent the same type of purification), almost up to the level

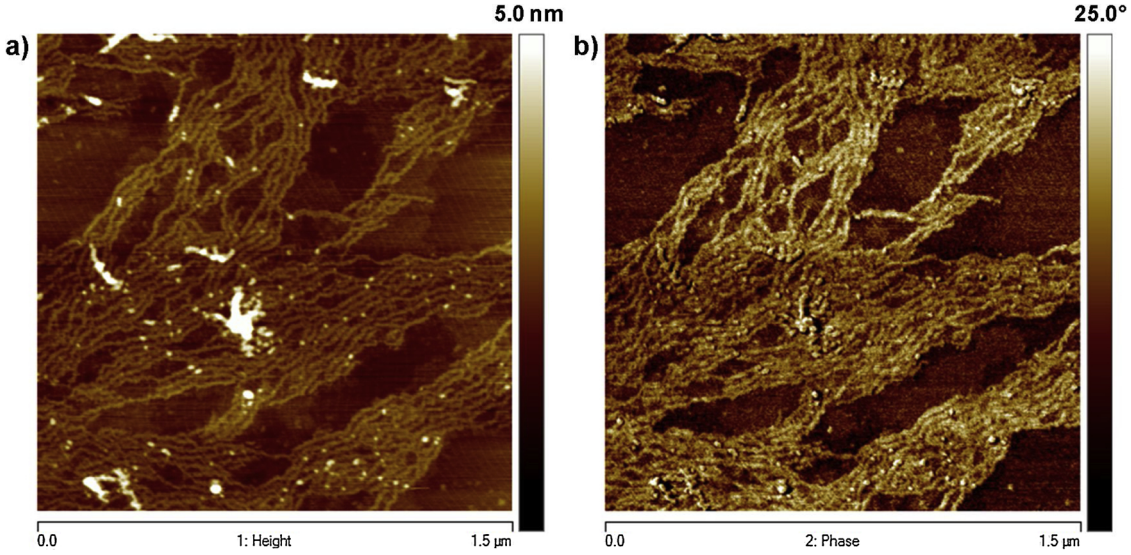

Fig. 4. 1.5 × 1.5 µm^2 height (a) and phase (b) AFM images of a thin film of P3HT-*b*-PFPE-*b*-P3HT block copolymer cast from a xylene solution.

Table 1
Photovoltaic performance of P3 H T (synthesized in this work and a commercial batch from Solarmer) and P3HT-*b*-PFPE-*b*-P3HT when employed as active layer component (V_{oc}: open-circuit voltage, J_{sc}: short-circuit current density, FF: fill factor and PCE: power conversion efficiency). Average PCEs were taken over 5–6 cells.

Active layer	M_w of the polymer (g. mol^{-1})	V_{OC} (V)	J_{SC} (mA cm^{-2})	FF	Average PCE (%)	Best PCE (%)
P3HT(synth):$PC_{61}BM$	31 000	0.48	5.98 ± 0.32	0.65	1.85 ± 0.13	2.05
P3HT-*b*-PFPE-*b*-P3HT:$PC_{61}BM$	36 600	0.52	7.69 ± 0.25	0.70	2.79 ± 0.14	2.99
P3HT(Sol.):$PC_{61}BM$	50 000-70 000	0.55	7.80 ± 0.39	0.73	3.14 ± 0.18	3.29

of commercial P3HT. The lower power conversion efficiency (PCE) for synthesized P3HT than commercial one may be in part explained by the presence of metal residues, which act as charge carrier traps and consequently, reduce the photovoltaic performance. [67] External quantum efficiencies (EQEs) of the top performing devices were also measured (Figure S10 in the Supporting Information). The shape of the spectra recorded for all three polythiophene materials is quite similar (absence of additional absorption at a different wavelength) and only the absolute EQE values in the range of 450 to 650 nm differ.

4. Conclusions

A ABA triblock copolymer based on π-conjugated P3HT segments and a fluorinated non-conjugated sequence was successfully synthesized. First, P3HT functionalized with an ethynyl end group was prepared using Kumada catalyst-transfer condensative polymerization. Then, this ethynyl end-functionalized P3HT was covalently coupled to a telechelic bisazido perfluopolyether (PFPE) via Huisgen click chemistry to afford the P3HT-*b*-PFPE-b-P3HT triblock copolymer. The copolymer thin films show a periodic P3HT nanofibril morphology with crystallites with “edge-on” orientation of the polymer chains. Modifying P3HT with the attachment of a soft PFPE segment allows to (almost) retain the favorable photovoltaic parameters when blended with $PC_{61}BM$. To go further, the impact of the molecular weight and the weight ratio of the PFPE segment on the solid-state morphologies and electrical properties will be systematically investigated. This work is currently in progress.

Declaration of interest

All author declare no conflict of interest.

Acknowledgments

The authors thank the CNRS and the Université de Montpellier for financial support. Research in Mons is supported by the FNRS Excellence of Science program (Precision and 2Dto3D projects, FNRS-FRFC and the ‘Actions de Recherche Concertée’ program (MADSSCELLS project). M.S. is a research associate of the FNRS. The FNRS is also acknowledged for a visiting professor grant for S.C. The UMons MS laboratory acknowledges the F.R.S.-FNRS for the acquisition of the Waters QToF Premier mass spectrometer and for continuing support. W.P. acknowledges the National Science Centre, Poland, through the grant UMO-2015/18/E/ST3/00322. The UHasselt co-authors thank the Research Foundation – Flanders (FWO – Vlaanderen) and Hasselt University for continuous financial support.

Appendix A. Supplementary data

Supplementary material related to this article can be found, in the online version, at doi:https://doi.org/10.1016/j.synthmet.2019.04.001.

References

[1] A.J. Heeger, Semiconducting polymers: the third generation, Chem. Soc. Rev. 39 (2010) 2354–2371.
[2] A.C. Grimsdale, K. Leok Chan, R.E. Martin, P.G. Jokisz, A.B. Holmes, Synthesis of light-emitting conjugated polymers for applications in electroluminescent devices, Chem. Rev. 109 (2009) 897–1091.
[3] C. Wang, H. Dong, W. Hu, Y. Liu, D. Zhu, Semiconducting π-Conjugated systems in field-effect transistors: a material odyssey of organic electronics, Chem. Rev. 112 (2012) 2208–2267.
[4] X. Guo, M. Baumgarten, K. Müllen, Designing π-conjugated polymers for organic electronics, Prog. Polym. Sci. 38 (2013) 1832–1908.
[5] A. Marrocchi, D. Lanari, A. Facchetti, L. Vaccaro, Poly(3-hexylthiophene): synthetic methodologies and properties in bulk heterojunction solar cells, Energy Environ. Sci. 5 (2012) 8457–8474.
[6] A.T. Kleinschmidt, S.E. Root, D.J. Lipomi, Poly(3-hexylthiophene) (P3HT): fruit fly or outlier in organic solar cell research? J. Mater. Chem. A Mater. Energy Sustain. 5 (2017) 11396–11400.
[7] M. Chevrier, R. Di Ciuccio, O. Coulembier, P. Dubois, S. Richeter, A. Mehdi, S. Clément, Functionalization of P3HT-based hybrid materials for photovoltaic

applications, in: B.P. Chauhan (Ed.), NOvel Nanoscale Hybrid Materials, John Wiley & Sons, Hoboken, NJ, 2018.
[8] A. Wadsworth, Z. Hamid, M. Bidwell, R.S. Ashraf, J.I. Khan, D.H. Anjum, C. Cendra, J. Yan, E. Rezasoltani, A.A.Y. Guilbert, M. Azzouzi, N. Gasparini, J.H. Bannock, D. Baran, H. Wu, J.C. de Mello, C.J. Brabec, A. Salleo, J. Nelson, F. Laquai, I. McCulloch, Progress in poly (3-hexylthiophene) organic solar cells and the influence of its molecular weight on device performance, Adv. Energy Mater. 8 (2018) 1801001.
[9] T. Yokozawa, Y. Nanashima, H. Kohno, R. Suzuki, M. Nojima, Y. Ohta, Catalyst-transfer condensation polymerization for precision synthesis of π-conjugated polymers, Pure Appl. Chem. (2012), p. 573.
[10] S. Agbolaghi, S. Zenoozi, A comprehensive review on poly(3-alkylthiophene)-based crystalline structures, protocols and electronic applications, Org. Electron. 51 (2017) 362–403.
[11] F.P.V. Koch, J. Rivnay, S. Foster, C. Müller, J.M. Downing, E. Buchaca-Domingo, P. Westacott, L. Yu, M. Yuan, M. Baklar, Z. Fei, C. Luscombe, M.A. McLachlan, M. Heeney, G. Rumbles, C. Silva, A. Salleo, J. Nelson, P. Smith, N. Stingelin, The impact of molecular weight on microstructure and charge transport in semicrystalline polymer semiconductors–poly(3-hexylthiophene), a model study, Prog. Polym. Sci. 38 (2013) 1978–1989.
[12] M.W. Matsen, F.S. Bates, Unifying weak- and Strong-segregation block copolymer theories, Macromolecules 29 (1996) 1091–1098.
[13] F.S. Bates, G.H. Fredrickson, Block copolymer thermodynamics: theory and experiment, Annu. Rev. Phys. Chem. 41 (1990) 525–557.
[14] J. Liu, E. Sheina, T. Kowalewski, R.D. McCullough, Tuning the electrical conductivity and self-assembly of regioregular polythiophene by block copolymerization: nanowire morphologies in new Di- and triblock copolymers, Angew. Chem. Int. Ed. 41 (2002) 329–332.
[15] E. Kaul, V. Senkovskyy, R. Tkachov, V. Bocharova, H. Komber, M. Stamm, A. Kiriy, Synthesis of a bifunctional initiator for controlled Kumada catalyst-transfer polycondensation/nitroxide-mediated polymerization and preparation of poly(3-hexylthiophene) – polystyrene block copolymer therefrom, Macromolecules 43 (2010) 77–81.
[16] A. Britze, V. Möllmann, G. Grundmeier, H. Luftmann, D. Kuckling, Synthesis of blockcopolymers P3HT-b-PS using a combination of Grignard-metathesis and nitroxide-mediated radical polymerization, Macromol. Chem. Phys. 212 (2011) 679–690.
[17] Z.-P. Yu, C.-H. Ma, Q. Wang, N. Liu, J. Yin, Z.-Q. Wu, Polyallene-block-polythiophene-block-polyallene copolymers: one-pot synthesis, helical assembly, and multiresponsiveness, Macromolecules 49 (2016) 1180–1190.
[18] F. Ge, Z. Liu, F. Tian, Y. Du, L. Liu, X. Wang, H. Lu, Z. Wu, G. Zhang, L. Qiu, One-pot synthesized ABA tri-block copolymers for high-performance organic field-effect transistors, Polym. Chem. 9 (2018) 4517–4522.
[19] L. Pessoni, J. De Winter, M. Surin, N. Hergué, N. Delbosc, R. Lazzaroni, P. Dubois, P. Gerbaux, O. Coulembier, Synthesis of polyphthalaldehyde-based block copolymers: utilization of a thermo-sacrificial segment for an easy access to fine-tuned poly(3-hexylthiophene) nanostructured films, Macromolecules 49 (2016) 3001–3008.
[20] H.C. Moon, A. Anthonysamy, J.K. Kim, A. Hirao, Facile synthetic route for well-defined poly(3-hexylthiophene)-block-poly(methyl methacrylate) copolymer by anionic coupling reaction, Macromolecules 44 (2011) 1894–1899.
[21] J.B. Gilroy, D.J. Lunn, S.K. Patra, G.R. Whittell, M.A. Winnik, I. Manners, Fiber-like micelles via the crystallization-driven solution self-assembly of poly(3-hexylthiophene)-block-Poly(methyl methacrylate) copolymers, Macromolecules 45 (2012) 5806–5815.
[22] E. Ji, V. Pellerin, L. Rubatat, E. Grelet, A. Bousquet, L. Billon, Self-assembly of Ionizable “clicked” P3HT-b-PMMA copolymers: ionic bonding group/counterion effects on morphology, Macromolecules 50 (2017) 235–243.
[23] R.H. Lohwasser, M. Thelakkat, Synthesis of amphiphilic rod–coil P3HT-b-P4VP carrying a long conjugated block using NMRP and click chemistry, Macromolecules 45 (2012) 3070–3077.
[24] V. Gernigon, P. Lévêque, F. Richard, N. Leclerc, C. Brochon, C.H. Braun, S. Ludwigs, D.V. Anokhin, D.A. Ivanov, G. Hadziioannou, T. Heiser, Microstructure and optoelectronic properties of P3HT-b-P4VP/PCBM blends: impact of PCBM on the copolymer self-assembly, Macromolecules 46 (2013) 8824–8831.
[25] M. Surin, O. Coulembier, K. Tran, J.D. Winter, P. Leclère, P. Gerbaux, R. Lazzaroni, P. Dubois, Regioregular poly(3-hexylthiophene)-poly(ε-caprolactone) block copolymers: Controlled synthesis, microscopic morphology, and charge transport properties, Org. Electron. 11 (2010) 767–774.
[26] G. Grancharov, O. Coulembier, M. Surin, R. Lazzaroni, P. Dubois, Stereocomplexed materials based on poly(3-hexylthiophene)-b-poly(lactide) block copolymers: synthesis by organic catalysis, thermal properties, and microscopic morphology, Macromolecules 43 (2010) 8957–8964.
[27] K. Tsuchiya, K. Ando, T. Shimomura, K. Ogino, Synthesis and characterization of poly(3-hexylthiophene)-block-poly(dimethylsiloxane) for photovoltaic application, Polymer 92 (2016) 125–132.
[28] P.M. Reichstein, S. Gödrich, G. Papastavrou, M. Thelakkat, Influence of composition of amphiphilic double-crystalline P3HT-b-PEG block copolymers on structure formation in aqueous solution, Macromolecules 49 (2016) 5484–5493.
[29] H. Erothu, A.A. Sohdi, A.C. Kumar, A.J. Sutherland, C. Dagron-Lartigau, A. Allal, R.C. Hiorns, P.D. Topham, Facile synthesis of poly(3-hexylthiophene)-block-poly (ethylene oxide) copolymers via Steglich esterification, Polym. Chem. 4 (2013) 3652–3655.
[30] S. Kang, R.J. Ono, C.W. Bielawski, Synthesis of poly(3-hexylthiophene)-block-poly (ethylene)-block-poly(3-hexylthiophene) via a combination of ring-opening olefin metathesis polymerization and grignard metathesis polymerization, J. Polym. Sci. A Polym. Chem. 51 (2013) 3810–3817.
[31] J. Brazard, R.J. Ono, C.W. Bielawski, P.F. Barbara, D.A. Vanden Bout, Mimicking conjugated polymer thin-film photophysics with a well-defined triblock copolymer in solution, J. Phys. Chem. B 117 (2013) 4170–4176.
[32] R. Peng, B. Pang, D. Hu, M. Chen, G. Zhang, X. Wang, H. Lu, K. Cho, L. Qiu, An ABA triblock copolymer strategy for intrinsically stretchable semiconductors, J. Mater, Chem. C 3 (2015) 3599–3606.
[33] F. Babudri, G.M. Farinola, F. Naso, R. Ragni, Fluorinated organic materials for electronic and optoelectronic applications: the role of the fluorine atom, Chem. Commun. (2007) 1003–1022.
[34] S. Clément, F. Meyer, J. De Winter, O. Coulembier, C.M.L. Vande Velde, M. Zeller, P. Gerbaux, J.-Y. Balandier, S. Sergeyev, R. Lazzaroni, Y. Geerts, P. Dubois, Synthesis and supramolecular organization of regioregular polythiophene block oligomers, J. Org. Chem. 75 (2010) 1561–1568.
[35] V.S.D. Voet, G. ten Brinke, K. Loos, Well-defined copolymers based on poly(vinylidene fluoride): from preparation and phase separation to application, J. Polym. Sci. A Polym. Chem. 52 (2014) 2861–2877.
[36] F. Meyer, Fluorinated conjugated polymers in organic bulk heterojunction photovoltaic solar cells, Prog. Polym. Sci. 47 (2015) 70–91.
[37] C.M. Friesen, B. Améduri, Outstanding telechelic perfluoropolyalkylethers and applications therefrom, Prog. Polym. Sci. 81 (2018) 238–280.
[38] J. Liu, D. Haynes, C. Balliet, R. Zhang, T. Kowalewski, R.D. McCullough, Self encapsulated poly(3-hexylthiophene)-poly(fluorinated alkyl methacrylate) rod-coil block copolymers with high field effect mobilities on bare SiO2, Adv. Funct. Mater. 22 (2012) 1024–1032.
[39] B. Lim, J. Jo, S.-I. Na, J. Kim, S.-S. Kim, D.-Y. Kim, A morphology controller for high-efficiency bulk-heterojunction polymer solar cells, J. Mater. Chem. 20 (2010) 10919–10923.
[40] J.S. Kim, Y. Lee, J.H. Lee, J.H. Park, J.K. Kim, K. Cho, High-efficiency organic solar cells based on end-functional-goup-modified poly(3-hexylthiophene), Adv. Mater. 22 (2010) 1355–1360.
[41] Z. Jia, G. Xu, Q. Li, Y. Zhang, B. Liu, Y. Pan, X. Wang, T. Wang, F. Li, Boosting the efficiency and stability of polymer solar cells using poly(3-hexylthiophene)-based all-conjugated diblock copolymers containing pentafluorophenyl groups, J. Mater. Sci. Mater. Electron. 29 (2018) 10337–10345.
[42] Y. Zhang, K. Tajima, K. Hirota, K. Hashimoto, Synthesis of all-conjugated diblock copolymers by quasi-living polymerization and observation of their microphase separation, J. Am. Chem. Soc. 130 (2008) 7812–7813.
[43] U. Beckmann, G. Hägele, W. Frank, Square-planar 2-toluenido(triphenylphosphane) nickel(ii) complexes containing bidentate N,O ligands: an example of planar chirality, Eur. J. Inorg. Chem. 2010 (2010) 1670–1678.
[44] N.H. Park, G. Teverovskiy, S.L. Buchwald, Development of an air-stable nickel precatalyst for the amination of aryl chlorides, sulfamates, mesylates, and triflates, Org. Lett. 16 (2014) 220–223.
[45] G. Lopez, M. Guerre, J. Schmidt, Y. Talmon, V. Ladmiral, J.-P. Habas, B. Améduri, An amphiphilic PEG-b-PFPE-b-PEG triblock copolymer: synthesis by CuAAC click chemistry and self-assembly in water, Polym. Chem. 7 (2016) 402–409.
[46] G. Lopez, B. Améduri, J.-P. Habas, A perfluoropolyether-based elastomers library with on-demand thermorheological features, Eur. Polym. J. 95 (2017) 207–215.
[47] M. Chevrier, S. Richeter, O. Coulembier, M. Surin, A. Mehdi, R. Lazzaroni, R.C. Evans, P. Dubois, S. Clément, Expanding the light absorption of poly(3-hexylthiophene) by end-functionalization with π-extended porphyrins, Chem. Commun. 52 (2016) 171–174.
[48] F. Boon, S. Desbief, L. Cutaia, O. Douhéret, A. Minoia, B. Ruelle, S. Clément, O. Coulembier, J. Cornil, P. Dubois, R. Lazzaroni, Synthesis and characterization of nanocomposites based on functional regioregular poly(3-hexylthiophene) and multiwall carbon nanotubes, Macromol. Rapid Commun. 31 (2010) 1427–1434.
[49] J. De Winter, G. Deshayes, F. Boon, O. Coulembier, P. Dubois, P. Gerbaux, MALDI-ToF analysis of polythiophene: use of trans-2-[3-(4-t-butyl-phenyl)-2-methyl- 2-propenylidene]malononitrile—DCTB—as matrix, J. Mass Spectrom. 46 (2011) 237–246.
[50] H.A. Bronstein, C.K. Luscombe, Externally initiated regioregular P3HT with controlled molecular weight and narrow polydispersity, J. Am. Chem. Soc. 131 (2009) 12894–12895.
[51] D. Schiefer, R. Hanselmann, M. Sommer, All-conjugated P3HT donor PCDTBT acceptor graft copolymers synthesised via a grafting through approach, Polym. Chem. 8 (2017) 4368–4377.
[52] Z. Li, R.J. Ono, Z.-Q. Wu, C.W. Bielawski, Synthesis and self-assembly of poly(3-hexylthiophene)-block-poly(acrylic acid), Chem. Commun. 47 (2011) 197–199.
[53] J. Liu, R.S. Loewe, R.D. McCullough, Employing MALDI-MS on poly(alkylthiophenes): analysis of molecular weights, molecular weight distributions, end-group structures, and end-group modifications, Macromolecules 32 (1999) 5777–5785.
[54] A. Rodrigues, M.C.R. Castro, A.S.F. Farinha, M. Oliveira, J.P.C. Tomé, A.V. Machado, M.M.M. Raposo, L. Hilliou, G. Bernardo, Thermal stability of P3HT and P3HT:PCBM blends in the molten state, Polymer Test. 32 (2013) 1192–1201.
[55] R. Ramani, J. Srivastava, S. Alam, Application of model-free kinetics to the thermal and thermo-oxidative degradation of poly(3-hexyl thiophene), Thermochim. Acta 499 (2010) 34–39.
[56] P. Kohn, S. Huettner, H. Komber, V. Senkovskyy, R. Tkachov, A. Kiriy, R.H. Friend, U. Steiner, W.T.S. Huck, J.-U. Sommer, M. Sommer, On the role of single regiodefects and polydispersity in regioregular poly(3-hexylthiophene): Defect distribution, synthesis of defect-free chains, and a simple model for the determination of crystallinity, J. Am. Chem. Soc. 134 (2012) 4790–4805.
[57] Y. Yuan, J. Zhang, J. Sun, J. Hu, T. Zhang, Y. Duan, Polymorphism and structural transition around 54 °C in regioregular poly(3-hexylthiophene) with high crystallinity as revealed by infrared spectroscopy, Macromolecules 44 (2011) 9341–9350.

[58] A. Priola, R. Bongiovanni, G. Malucelli, A. Pollicino, C. Tonelli, G. Simeone, UV-curable systems containing perfluoropolyether structures: synthesis and characterisation, Macromol. Chem. Phys. 198 (2003) 1893–1907.
[59] W.D. Oosterbaan, V. Vrindts, S. Berson, S. Guillerez, O. Douhéret, B. Ruttens, J. D'Haen, P. Adriaensens, J. Manca, L. Lutsen, D. Vanderzande, Efficient formation, isolation and characterization of poly(3-alkylthiophene) nanofibres: probing order as a function of side-chain length, J. Mater. Chem. 19 (2009) 5424–5435.
[60] M. Sundberg, O. Inganäs, S. Stafström, G. Gustafsson, B. Sjögren, Optical absorption of poly(3-alkylthiophenes) at low temperatures, Solid State Commun. 71 (1989) 435–439.
[61] D.T. Duong, C. Wang, E. Antono, M.F. Toney, A. Salleo, The chemical and structural origin of efficient p-type doping in P3HT, Org. Electron. 14 (2013) 1330–1336.
[62] E. Lim, K.A. Peterson, G.M. Su, M.L. Chabinyc, Thermoelectric properties of poly(3-hexylthiophene) (P3HT) doped with 2,3,5,6-tetrafluoro-7,7,8,8-tetra-cyanoquinodimethane (F4TCNQ) by vapor-phase infiltration, Chem. Mater. 30 (2018) 998–1010.
[63] Y.-H. Lin, K.G. Yager, B. Stewart, R. Verduzco, Lamellar and liquid crystal ordering in solvent-annealed all-conjugated block copolymers, Soft Matter 10 (2014) 3817–3825.
[64] H. Yang, T.J. Shin, L. Yang, K. Cho, C.Y. Ryu, Z. Bao, Effect of mesoscale crystalline structure on the field-effect mobility of regioregular poly(3-hexyl thiophene) in thin-film transistors, Adv. Funct. Mater. 15 (2005) 671–676.
[65] M. Surin, P. Leclère, R. Lazzaroni, J.D. Yuen, G. Wang, D. Moses, A.J. Heeger, S. Cho, K. Lee, Relationship between the microscopic morphology and the charge transport properties in poly(3-hexylthiophene) field-effect transistors, J. Appl. Phys. 100 (2006) 033712.
[66] S. Berson, R. De Bettignies, S. Bailly, S. Guillerez, Poly(3-hexylthiophene) fibers for photovoltaic applications, Adv. Funct. Mater. 17 (2007) 1377–1384.
[67] Ö. Usluer, M. Abbas, G. Wantz, L. Vignau, L. Hirsch, E. Grana, C. Brochon, E. Cloutet, G. Hadziioannou, Metal residues in semiconducting polymers: impact on the performance of organic electronic devices, ACS Macro Lett. 3 (2014) 1134–1138.